THE JOURNAL OF PHYSICAL CHEMISTRY C
A JOURNAL OF THE AMERICAN CHEMICAL SOCIETY

pubs.acs.org/JPCC

Article

# Impact of Nanostructurization of the Pore Walls on the Dynamics of a Series of Phenyl Alcohols Incorporated within Nanoporous Aluminum Oxide Templates

Adam Górny, Magdalena Tarnacka,* Sara Zimny, Monika Geppert-Rybczyńska, Agnieszka Brzózka, Grzegorz D. Sulka, Marian Paluch, and Kamil Kamiński

Cite This: *J. Phys. Chem. C* 2022, 126, 18475−18489

Read Online

ACCESS | Metrics & More | Article Recommendations | Supporting Information

**ABSTRACT:** Herein, we studied the impact of surface roughness on the molecular dynamics of a series of phenyl-terminated monohydroxyalcohols under spatial confinement provided by nanoporous anodic aluminum oxide (AAO) membranes of constant (const-AAO) and modulated (modul-AAO) pore diameter using Broadband Dielectric Spectroscopy and Differential Scanning Calorimetry. Interestingly, we observed that both types of AAO membranes affect the behavior of examined associating materials in a different manner. Calorimetric measurements showed that the double glass transition phenomenon, commonly reported for many compounds infiltrated into const-AAO membranes, is not observed in the case of modul-AAO templates, where a single glass transition temperature was detected. Consequently, the dynamics of the dominant process was bulk-like in the whole range of studied temperatures for the samples infiltrated into the latter templates. Moreover, the Debye character of the dominant relaxation process characteristic for bulk samples was lost for the confined samples. Interestingly, the width of the dominant mode was the greatest in the alcohols infiltrated into modulated pores. It was assigned to the higher heterogeneity in the mobility introduced by the nanostructurization of the interface. The presented data emphasize the crucial impact of modulated-induced surface roughness of an applied constrained medium on the dynamics and phase transition of the liquids infiltrated into pores.

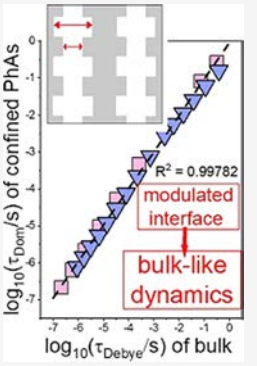


## I. INTRODUCTION

Monohydroxy alcohols (monoalcohols, MA), containing a single hydroxyl group (−OH) being the major source of their dipole moment, represent a group of amphiphilic compounds, i.e., having both the hydrophilic (−OH) and hydrophobic (aliphatic chain) parts. The other interesting issue worth emphasizing is the fact that it is relatively easy to modify the structure and geometry of molecules within the nonpolar part (change of length, rigidity or branching of the aliphatic chain, addition of steric hindrance) and the polar part (changing the number and position of hydroxyl groups or adding another polar moiety). Moreover, these materials can be easily supercooled, so we can study their behavior in a wide range of temperatures and pressures. All these features allow us to classify monohydroxy alcohols as a convenient model to study the self-assembly phenomenon, driven mainly by noncovalent interactions such as hydrogen bonds, steric effects, electrostatic interactions, or hydrophobic and hydrophilic effects.[1−3] Consequently, the impact of different factors on the self-assembly phenomenon, architecture of aggregates, and mechanism of their formation can be gained. These clear advantages of MA resulted in publication of numerous articles on these systems where different experimental and theoretical methods including broadband dielectric spectroscopy were applied.[2,4−9] However, these investigations mostly focus on aliphatic monoalcohols in the bulk phase.

In general, the dielectric spectra of glass-forming liquids exhibit primary structural ($\alpha$) relaxation with the possible presence of faster secondary relaxation processes. Importantly, the dielectric response of the majority of the systems studied so far is nonexponential (non-Debye).[10,11] On the other hand, in spectra of monoalcohols collected in the supercooled liquid state, one can observe the presence of a prominent, symmetric Debye peak, whereas the $\alpha$-process often manifests itself as an excess wing in the high-frequency region.[2,4,12,13] The nature of the Debye (D) process in MA has been studied over many years in order to find its molecular origin.[2] However, recent studies have clearly shown that this D-mode originates from the formation of transient chains (molecules can join and leave the chain) via hydrogen bonds. These structures, by analogy to the type-A polymers, are characterized by a dipole moment parallel to the backbone. Therefore, the fluctuation in the dipole moment due to attachment or detachment of the single molecule to the transient chain gives rise to variation in

Received: August 1, 2022
Revised: October 7, 2022
Published: October 21, 2022







https://doi.org/10.1021/acs.jpcc.2c05446
*J. Phys. Chem. C* 2022, 126, 18475−18489

**Scheme 1. Chemical Structures of Investigated Phenyl Alcohols**

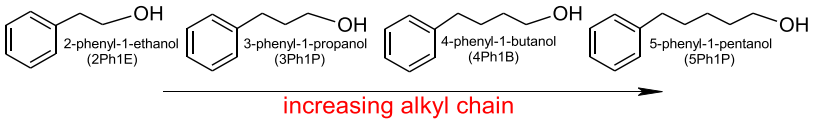


**Scheme 2. Drawings of a Schematic (a) Top-View and (b, c) Cross-Section of const-AAO (b) and modul-AAO (c) Templates**

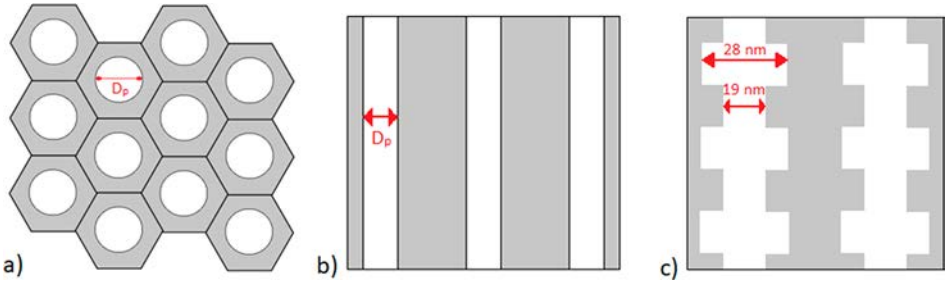


polarization and appearance of the Debye response in loss spectra.[4,13] The dynamical parameters describing this puzzling relaxation process depends on the structure of the alcohol molecule itself, i.e., a number of −OH groups and particularly their mutual arrangement, which can lead to the formation of other (nonlinear) hydrogen bonded supramolecular structures.[2,13,14] Moreover, they can be used to make some conclusions about the self-association in the investigated system. It was shown that the higher stiffness of the alcohol molecule, resulting from the addition of a phenyl ring, significantly hinders the self-assembling process, which results in a smaller size of hydrogen-bonded clusters.[4,15,16] The formation of hydrogen bonds can be even completely suppressed, especially when the steric hindrance is located in the vicinity of hydroxyl group (i.e., 1-phenyl-1-propanol), which is then reflected in the amplitude of the Debye process.[17] Pressure studies also show that elevated pressure affects the hydrogen bonding network structure in monoalcohols, yet the exact mechanism remains unclear.[18−22]

Another, rather innovative, way to study molecular dynamics and thus structures that form at the atomic level is to apply a spatial confinement. Gainaru et al.[23] showed that for 2-ethyl-1-hexanol (2E1H), confined within the surface of collagen matrix at different concentrations, a prominent Debye-like process becomes broader non-Debye as the alcohol concentration decreases. At the same time, an increase in the relative strength of structural relaxation was observed, associated with a decreasing population of supramolecular structures. Ultimately, it was even possible to reach the state of nonassociating liquid. Another approach to nanospatical restriction of the sample is the use of a hard confinement (in the form of nanopores), which also allows us to modify this effect further by changing the diameter of the nanochannels, the type of material they are made of, their volume or shape. Ananiadou et al.[14] showed that for monohydroxy alcohols infiltrated into nanoporous alumina templates, the average dielectric strength of Debye-like relaxation is reduced, which is associated with a lower number of hydrogen bonds, resulting further in faster dynamics. They also observed that the number of molecules forming hydrogen-bonded linear structures decreases with decreasing pore diameter (from 7 in the bulk to 2 in 25 nm pores for 2E1H). A similar effect was obtained by Kipnusu et al.[24] and Talik et al.[25] for primary alcohols confined in silica templates of pore size, $D_p$ = 4 nm. In the same paper, they also concluded that the hydrogen bonds become weaker and inhomogeneous under spatial restriction.

In this paper, we investigated the impact of nanoscale confinement on the behavior of four phenyl-terminated monohydroxyalcohols (phenyl alcohols, PhAs), 2-phenyl-1-ethanol (2Ph1E), 3-phenyl-1-propanol (3Ph1P), 4-phenyl-1-butanol (4Ph1B), and 5-phenyl-1-pentanol (5Ph1P), that vary in the length of the alkyl chain (see Scheme 1), by means of Broadband Dielectric Spectroscopy (BDS) and Differential Scanning Calorimetry (DSC). The nanoscale confinement examined in this paper was produced by the two types of the porous anodic aluminum oxide (AAO) matrixes characterized by either (1) constant or (2) modulated pore diameter ($D_p$) of comparable sizes labeled herein as const-AAO and modul-AAO, respectively (see Scheme 2). Previous studies on the bulk materials revealed that many of their properties, i.e., the degree of association of molecules via hydrogen bonds, the association−dissociation energy, and the glass transition temperature ($T_g$), change depending on the length of the alkyl chain according to the "odd−even" effect.[26] This was discussed in terms of the interplay between interactions of the nonpolar and polar parts of the molecules, which was concluded to have a significant influence on the local structure and intra- and intermolecular dynamics of the studied PhAs. Therefore, it is interesting to see whether similar effects will be observed for the samples confined in mesoporous templates. It should be highlighted that to the best our knowledge, this is the first study on the impact of porous AAO matrices characterized by the modulated pore diameter on the behavior of low-molecular weight associating materials. Note that the modulated pore size of modul-AAO templates might be considered as an additional factor leading to an increase of roughness of inner pore walls.

## II. EXPERIMENTAL SECTION

**Materials.** Investigated phenyl alcohols ($C_6H_5-(CH_2)_n-OH$, $n$ = 2−5), with purity higher than 98%, were purchased from Sigma-Aldrich. Prior to use, the alcohols were heated ($T$ = 323 K) under a vacuum for about 20 min in order to remove residual water. The chemical structure of the alcohols studied is shown in Scheme 1.

In this study, we used the porous anodic aluminum oxide (AAO) membranes composed of uniaxial channels (open from both sides) with a well-defined pore diameter of the constant (const-AAO) or modulated (modul-AAO) value. Const-AAO



https://doi.org/10.1021/acs.jpcc.2c05446
J. Phys. Chem. C 2022, 126, 18475−18489

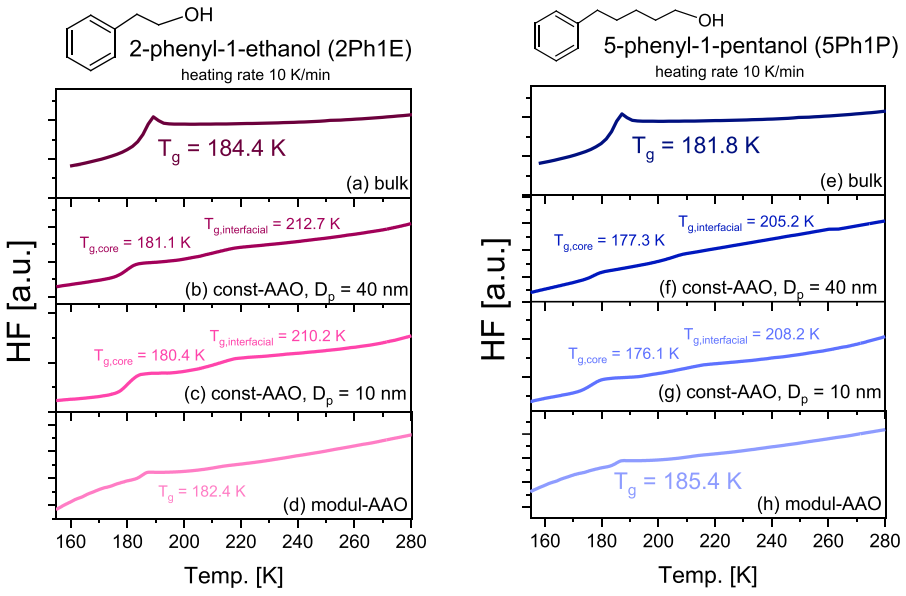


**Figure 1.** DSC thermograms obtained for bulk and confined samples of 2Ph1E (a–d) and 5Ph1P (e–h).

membranes were purchased from InRedox Technologies and were characterized by porous channels of pore diameters, $D_p$ = 10 and $D_p$ = 40 nm. On the other hand, modul-AAO membranes of modulated pore size ($D_p$ = 19 nm (mild anodizing mode) and $D_p$ = 28 nm (hard anodizing mode)) were prepared by the two-step anodization of aluminum in stirred 0.3 M $H_2SO_4$ at 5 °C.[27,28] The morphology of the applied membranes is shown in the Scheme 2. Details concerning the nanostructurization of inner walls of modul-AAO can be found in ref 28.

Before filling, all types of membranes were dried in an oven at $T$ = 423 K under a vacuum to remove any volatile impurities from the nanochannels. After cooling, they were used as a constrained medium. For that purpose, AAO templates were placed in a small glass flask containing examined MAs. The whole system was maintained at $T$ = 298 K in a vacuum ($10^{-2}$ bar) for $t$ = 5 h to let the samples flow into the nanocavities. Samples were finally annealed at $T$ = 353 K under a vacuum for $t$ = 1 h and weighed thereafter. The complete filling was obtained by a series of repeated infiltration procedure until the weight of the templates before and after was constant. After filling, the excess sample on the surface of the membranes was removed with a paper towel.

**Broadband Dielectric Spectroscopy (BDS).** BDS measurements were carried out on heating after a fast quenching of the liquid state in a wide range of temperatures ($T$ = 175–243 K) and frequencies ($f$ = $10^{-1}$–$10^{6}$ Hz) using a Novocontrol spectrometer, equipped with an Alpha Impedance Analyzer with an active sample cell and Quatro Cryosystem. Dielectric measurements of bulk samples were performed in a parallel-plate cell (diameter, 15 mm; gap, 0.1 mm) as described in ref 26. AAO membranes filled with studied alcohols were also placed in a similar capacitor (diameter, 10 mm; membrane thickness, 0.05 mm).[29,30] Nevertheless, the confined samples are a heterogeneous dielectric consisting of a matrix and an investigated compound. Because the applied electric field is parallel to the long pore axes, the equivalent circuit consists of two capacitors in parallel composed of $\varepsilon^*_{compound}$ and $\varepsilon^*_{AAO}$. Thus, the measured total impedance is related to the individual values through $1/Z^*_c = 1/Z^*_{compound} + 1/Z^*_{AAO}$, where the contribution of the matrix is marginal. The measured dielectric spectra were corrected according to the method presented in ref 31.

In order to obtain relaxation times ($\tau$) and also shape parameters of relaxation peaks, the dielectric data were fitted using the Havrilak–Negami (HN) function:[32]

$$\varepsilon(\bar{\omega})'' = \frac{\sigma_{DC}}{\varepsilon_0 \bar{\omega}} + \frac{\Delta\varepsilon}{[1 + (i\bar{\omega}\tau_{HN})^{\alpha_{HN}}]^{\beta_{HN}}} \quad (1)$$

where $\sigma_{DC}$ is the DC-conductivity term, $\varepsilon_0$ is the vacuum permittivity, $\bar{\omega}$ is angular frequency, $\tau_{HN}$ describes HN relaxation time, and $\alpha_{HN}$ and $\beta_{HN}$ are the shape parameters representing the symmetric and asymmetric broadening of given relaxation peaks.

**Differential Scanning Calorimetry (DSC).** Calorimetric measurements were carried out by a Mettler-Toledo DSC apparatus equipped with a liquid nitrogen cooling accessory and an HSS8 ceramic sensor (heat flux sensor with 120 thermocouples). Temperature and enthalpy calibrations were performed by using indium and zinc standards. The sample was prepared in an open aluminum crucible (40 $\mu$L) outside the DSC apparatus. Samples were scanned at various temperatures at a constant heating rate of 5, 10, and 20 K/min.

**Surface Tension and Contact Angle Measurements.** The surface tension of liquids $\gamma_L$ (pendant drop method) and contact angle $\theta$ were measured with a DSA 100S Krüss Tensiometer, GmbH Germany. The description of the instrument and procedures has been presented previously.[33,34] The measuring procedure at 298.2 K for all substances has been repeated a dozen or more times. The temperature measurements uncertainty was ±0.1 K. The precision of contact angle measurements was 0.01°, and the estimated uncertainty was ±1.5°, whereas the uncertainty of surface tension was ±0.1 mN/m. Density, $\rho$, required for the surface tension experiment was measured with an Anton Paar DMA 5000 M densimeter with the uncertainty not worse than 0.0001 g/cm$^3$.

## III. RESULTS AND DISCUSSION

Representative DSC thermograms obtained for two chosen bulk alcohols, 2-phenyl-1-ethanol (2Ph1E) and 5-phenyl-1-pentanol (5Ph1P), and samples infiltrated into various const- and modul-



https://doi.org/10.1021/acs.jpcc.2c05446
J. Phys. Chem. C 2022, 126, 18475–18489

**Table 1. Comparison of the Glass Transition Temperatures Obtained from BDS and DSC Measurements, for All Studied Samples (Both Bulk and Confined Ones)[a]**

| | DSC measurements | | BDS measurements | | | |
|---|---|---|---|---|---|---|
| sample | $T_{g,interfacial}$ [K] | $T_{g,core}$ [K] | $T_{g,interfacial}$ [K] | $T_{g,core}$ [K] | $\Delta T_{g,interfacial}$ [K] | $\Delta T_{g,core}$ [K] |
| | | | 2Ph1E | | | |
| bulk | | 184.4 | | 180.4 | | |
| $D_p$ = 40 nm | 212.7 | 181.1 | 199.2 | 172.2 | 18.8 | −8.1 |
| $D_p$ = 10 nm | 210.2 | 180.4 | 197.2 | 162.0 | 26.8 | −9.5 |
| modul-AAO | | 182.4 | | 178.6 | | −1.8 |
| | | | 3Ph1P | | | |
| bulk | | 181.9 | | 178.4 | | |
| $D_p$ = 40 nm | 205.1 | 175.9 | 197.2 | 162.0 | 18.8 | −16.4 |
| $D_p$ = 10 nm | 208.4 | 176.1 | 201.2 | 165.2 | 22.8 | −13.2 |
| modul-AAO | | 183.3 | | 173.8 | | −4.6 |
| | | | 4Ph1B | | | |
| bulk | | 180.9 | | 175.2 | | |
| $D_p$ = 40 nm | 200.5 | 175.9 | 195.2 | 159.9 | 20.0 | −15.3 |
| $D_p$ = 10 nm | 211.4 | 175.5 | 199.2 | 166.6 | 24.0 | −8.6 |
| modul-AAO | | 182.3 | | 173.9 | | −1.3 |
| | | | 5Ph1P | | | |
| bulk | | 181.8 | | 177.8 | | |
| $D_p$ = 40 nm | 205.2 | 177.3 | 197.2 | 160.8 | 19.3 | −17.0 |
| $D_p$ = 10 nm | 208.2 | 176.1 | 199.2 | 165.4 | 21.3 | −12.5 |
| modul-AAO | | 185.4 | | 174.2 | | −3.7 |

[a]The uncertainty of $T_g$ determination is ±2 K for all presented values.

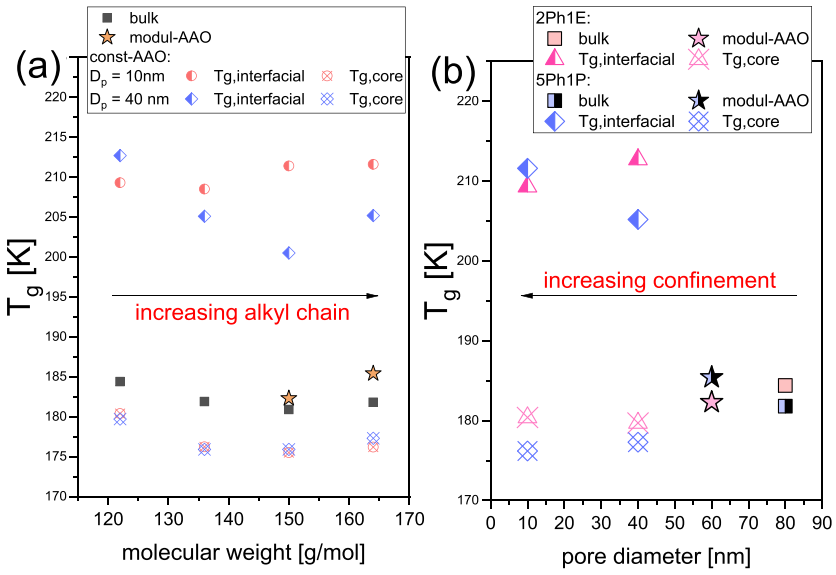


**Figure 2.** (a) Glass transition temperatures (determined from calorimetric measurements) of the bulk and confined sample vs molecular weight of PhA. (b) Glass transition temperatures determined from calorimetric measurements for 2Ph1E and 5Ph1P plotted vs pore diameter.

AAO membranes are shown in Figure 1. As can be seen for the bulk materials, they display the presence of one clear endothermic event related to the glass transition, characterized by a comparable values of the glass transition temperatures, $T_g$ (see Figure 1a,e). The determined values of glass transition temperatures for all systems are listed in Table 1. As previously discussed, this indicates that the elongation of the alkyl chain in the studied bulk PhAs does not significantly affect $T_g$.[26]

On the other hand, for samples infiltrated into AAO templates of various constant $D_p$ the scenario is quite different. For all those materials, we can observe two endothermic signals discussed in the literature as a so-called double glass transition (DGT) phenomenon where both $T_g$ values are located above and below the one observed for the bulk material independent of the molecular weight of PhAs and pore diameters (see Figure 1b,c and Figure 1f,g). One can recall that similar findings are commonly reported in the literature for various glass formers under confinement,[25,28,35−39] including materials able to create excessive hydrogen bonding structures. According to the "two-layer" (or "core-shell") model,[41,42] there are different types of interactions within infiltrated materials, which result in heterogeneity in terms of molecular dynamics as well as packing density.[24] Due to the interactions between the surface of the inner pore wall and the sample, the mobility of this "interfacial" molecules is slower compared to the ones located more in the middle of the nanochannels, labeled as the "core" fraction of


https://doi.org/10.1021/acs.jpcc.2c05446
J. Phys. Chem. C 2022, 126, 18475−18489

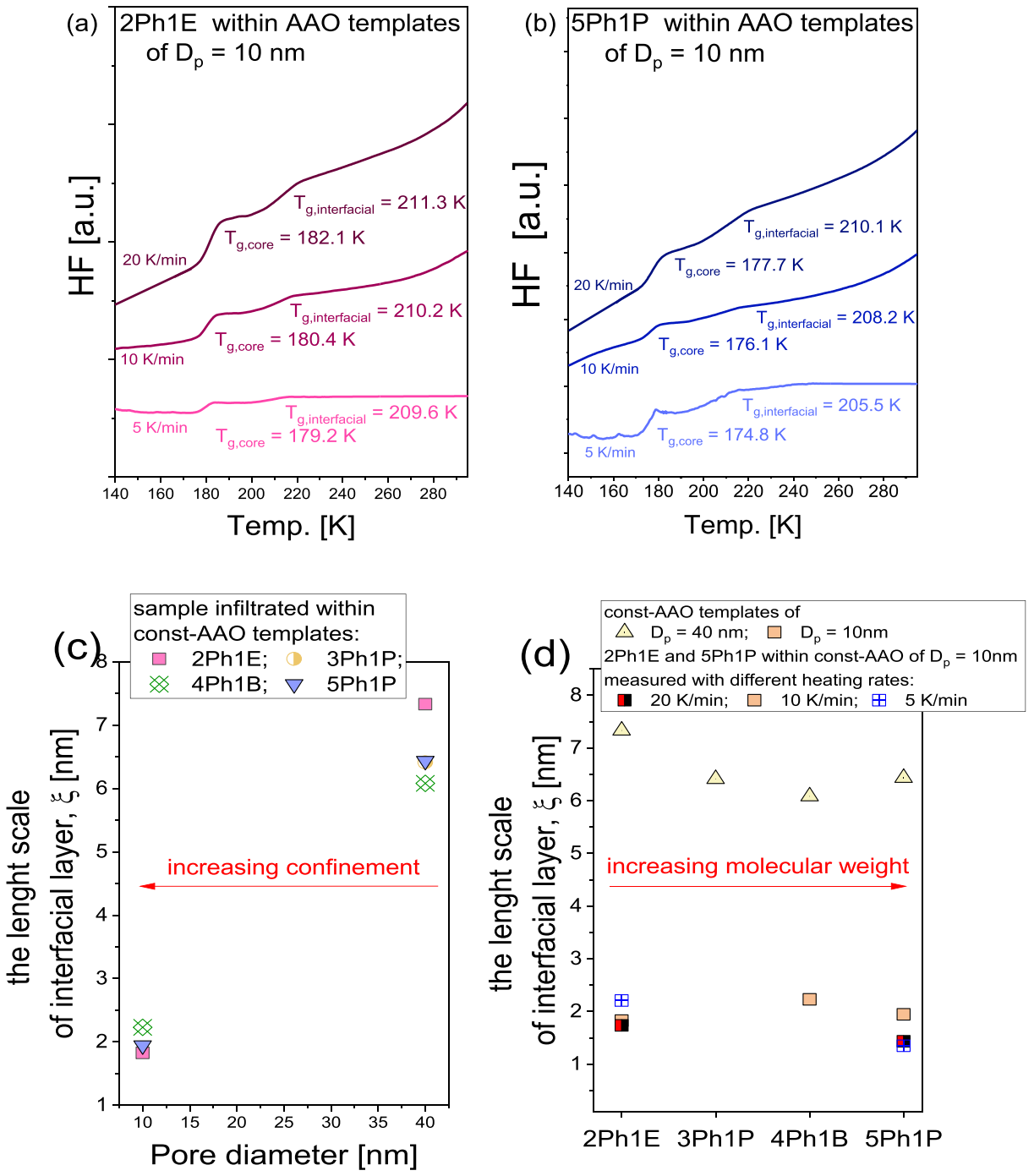


**Figure 3.** DSC thermograms for 2Ph1E (a) and 5Ph1P (b) confined in const-AAO templates of $D_p$ = 10 nm measured at different heating rates: 5/10/20 K/min. (c,d) Thickness of the interfacial layer ($\xi$) plotted versus the pore diameter (c) for PhAs within const-AAO templates the length of the alkyl chain (d).

more bulk-like molecules. The reduced mobility results in the glass transition occurring at higher temperatures ($T_{g,interfacial}$), whereas the core molecules are characterized by lower values of the glass transition temperatures ($T_{g,core}$). Interestingly, both $T_{g,interfacial}$ and $T_{g,core}$ change in a nonlinear manner with the elongation of the alkyl chain. However, it should be mentioned that although $T_{g,core}(M)$ changes similarly to the bulk for both examined $D_p$, interestingly, there is no difference between $T_{g,core}$ of samples infiltrated within const-AAO templates of $D_p$ = 10 nm and $D_p$ = 40 nm. On the other hand, in the case of $T_{g,interfacial}(M)$, one can see that it varies in a different way depending on the applied pore diameter; see Figure 2a. Note that, for $D_p$ = 40 nm, we can see a significant decrease in $T_{g,interfacial}$ from 2Ph1E to 4Ph1B and then a slight increase for 5Ph1P to the similar value to 3Ph1P, which is different than the trend observed for $T_{g,core}(M)$. This difference is even more pronounced in the pore diameter dependences of both $T_g$ values shown in Figure 2b. Herein, one can see that as the degree of confinement increases (pore diameter decreases) for const-AAO membranes, $T_{g,interfacial}$ either decreases or increases for 2Ph1E and 5Ph1P, respectively. In this context, one can mention that typical $T_{g,interfacial}$ increases and $T_{g,core}$ decreases in a linear manner with $D_p$ for infiltrated


https://doi.org/10.1021/acs.jpcc.2c05446
J. Phys. Chem. C 2022, 126, 18475−18489

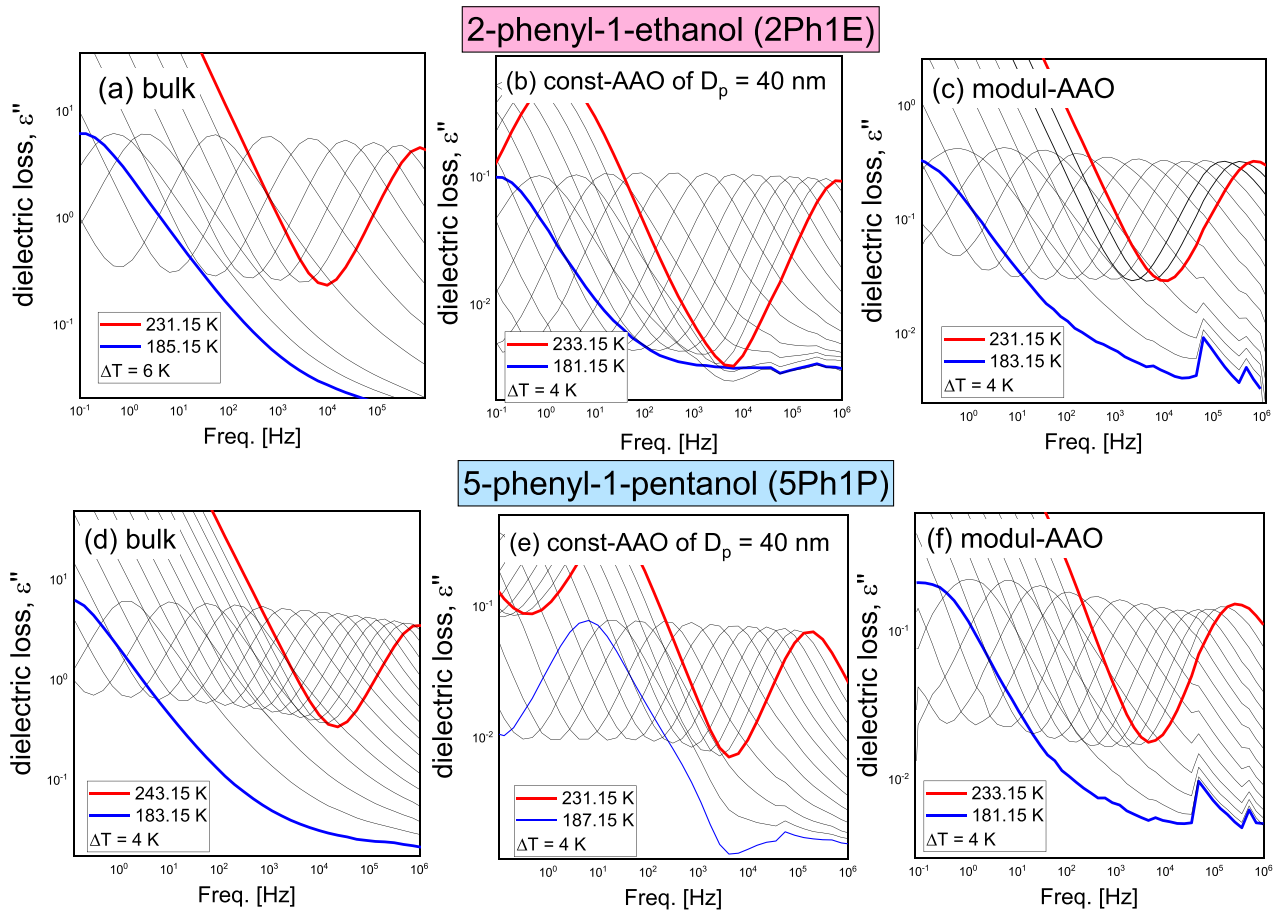


**Figure 4.** Dielectric loss spectra of 2Ph1E (a–c) and 5Ph1P (d–f) obtained for bulk systems (a, d) and also for alcohols confined in const-AAO templates of $D_p$ = 40 nm (b, e) and modul-AAO (c, f) membranes.

systems.[28,35,38,40] However, in our case, both $T_g$ values behave differently, which seem to be governed by the molecular weight of the examined PhAs.

In order to explain the impact of chemical structure on the observed differences in $T_{g,interfacial}$, we carried out a series of additional DSC measurements for 2Ph1E and 5Ph1P incorporated within const-AAO membranes of $D_p$ = 10 with different heating rates of 5, 10, and 20 K/min. As shown in Figure 3a,b, both $T_g$ values increase with an increasing heating rates, which agrees with the literature.[43,44] Furthermore, taking advantage of performed calorimetric measurements, we determined the length scale of interfacial layer ($\xi$) using the following equation:[41]

$$\xi = \frac{D_p}{2}\left[1 - \left(1 - \frac{\Delta C_{p,interfacial}}{\Delta C_{p,interfacial} + \Delta C_{p,core}}\right)^{1/2}\right] \quad (2)$$

where $\Delta C_{p,interfacial}$ and $\Delta C_{p,core}$ are heat capacity changes at $T_{g,interfacial}$ and $T_{g,core}$, respectively, and $D_p$ denotes the pore diameter. It is worthwhile to note that eq 2 can be used when the following conditions are fulfilled: the volume of the material in the surface layer is proportional to the step change of its heat capacity, the density of the confined sample is constant along the pore radius, and the pore is cylindrical. The values of $\xi$ calculated for all samples infiltrated into const-AAO templates plotted as a function of the alkyl chain and pore diameters are presented in Figure 3c,d, respectively. As observed, the thickness of interfacial layer oscillates around $\xi$ = 2 nm and $\xi$ = 6 nm for samples incorporated into templates of $D_p$ = 10 nm and $D_p$ = 40 nm, respectively. Note that the thickness of the interfacial layer determined for examined PhAs infiltrated within const-AAO templates of $D_p$ = 40 nm reaches $\xi \sim 6-7$ nm, which might indicate about 10 molecular layers. Taking into account that the studied PhAs are able to formed an extended H-bond network, we assume that this quite high value of $\xi$ is related to the associating structure formed by studied materials at the interface. This implies that the molecules are not densely packed, but they rather form various hoops and loops (of relatively big size) at the interface due to the intramolecular hydrogen bonding, resulting in $\xi \sim 6-7$ nm. Additionally, one can add that the applied model (eq 2) is a simple mathematical equation, assuming direct proportionality between the heat capacity and the number of molecules. It does not take into account any variation in the density or the heat capacity of the adsorbed molecules vs core ones. We think that these limitations of the applied model are the main source of overestimation of $\xi$. It is also worthwhile to mention that, in contrast to the thin films (planar surfaces), aside from this imperfect equation, there are no other tools allowing us to determine the thickness of the interfacial layer in the pores (strongly curved surface). It should be mentioned that obtained $\xi$ values are comparable to those determined for other associating materials, i.e., $\xi \approx 2.5-5.5$ nm for hydroxyl-terminated polypropylene glycol (PPG–OH) infiltrated into const-AAO templates of $D_p$ = 18–35 nm[36] and $\xi \approx 2.5-8$ nm for salol incorporated into const-AAO membranes of $D_p$ = 13–55 nm.[38] For comparison, one can



https://doi.org/10.1021/acs.jpcc.2c05446
J. Phys. Chem. C 2022, 126, 18475–18489

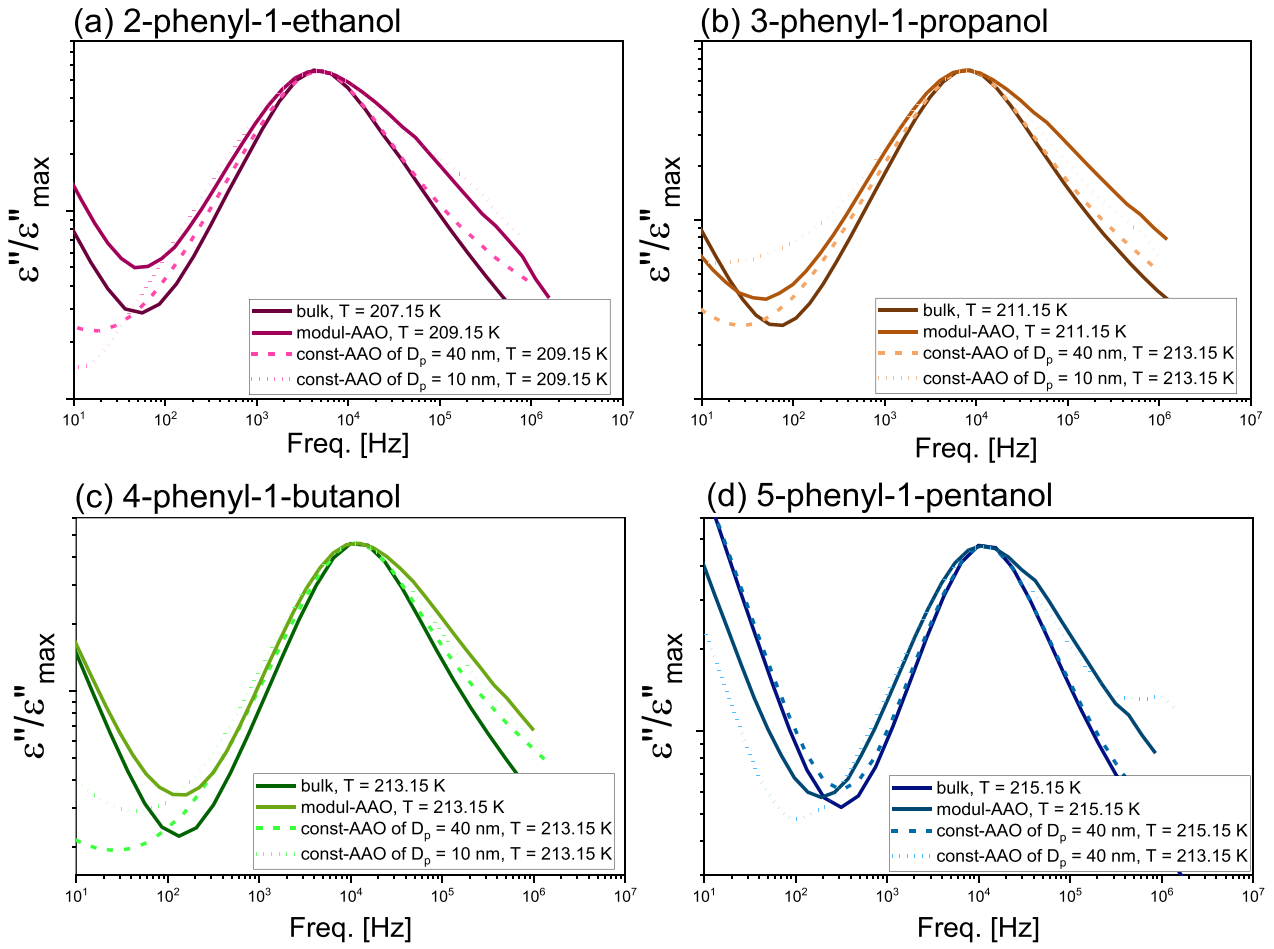


**Figure 5.** Comparison of dielectric loss peaks obtained for all measured samples at $f \approx 10$ kHz.

also mention that in the case of the primary and secondary monohydroxyalcohols, 2-ethyl-1-hexanol (2E1H), 2-ethyl-1-butanol (2E1B), and 5-methyl-3-heptanol (5M3H) infiltrated into native silica templates of $D_p = 4-8$ nm, the thickness of the interfacial layer reaches $\xi \approx 0.5-1.45$ nm (calculated from dielectric data).[25,30] In all mentioned cases, $\xi$ was reported to increase with increasing $D_p$.[36,38,40] This agrees with our data, where we can clearly see that the interfacial layer is around 3 times thicker for $D_p = 40$ nm than for $D_p = 10$ nm; see Figure 3c. Moreover, interestingly, there is only small variation in the interfacial layers formed by the examined PhAs with the elongation of the alkyl chain. Note that, for $D_p = 40$ nm, $\xi$ decreases with the length of the alkyl chain from 2Ph1E to 4Ph1B and then slightly increases for 5Ph1P to the similar level to 3Ph1P; see Figure 3d. In addition, $\xi$ seems to be also affected by heating rate values, where for 5 K/min, the highest and lowest values of $\xi$ were determined for 2Ph1E and 5Ph1P, respectively (Figure 3d). In this context, one can assume that observed differences in $T_{g,interfacial}$ between both samples result from a variation in the thickness of the interfacial layers due to the chemical structure of examined PhAs.

As mentioned above, the behavior of the examined series of PhAs infiltrated into AAO templates with the modulated pore diameter (modul-AAO) is completely different from the one observed in the case of applied const-AAO membranes. As shown in Figure 1d,h, we can see that recorded DSC signals reveal only one glass transition process (where $T_{g,modul} \sim T_{g,bulk}$) in contrast to those observed for PhAs incorporated within const-AAO, which exhibits two glass transitions. One can recall that such a phenomenon was also observed for a series of hydroxyl- and amino-terminated polypropylene glycols (PPG–OH and PPG-$NH_2$) of the molecular weight $M_n = 2000-4000$ g/mol incorporated into modulated alumina pores.[28] Combination of BDS, DSC, and FTIR measurements allowed us to conclude that the observed "bulk-like" behavior of confined series of PPG origins from the reduced surface interactions were due the modulation-induced roughness of the inner pore surface. Consequently, the interactions of PPGs and pore walls were weaker in templates of modulated pores with no well-defined interfacial layer when compared to const-AAO membranes, leading to the bulk-like behavior. Surprisingly, herein, we observed the same scenario, which seems to also suggest the absence or presence of very thin interfacial layer of PhAs molecules in these systems. Therefore, one can assume that the behavior of examined nanomaterials is dominated by the core bulk-like molecules for the sample incorporated into modul-AAO templates. Surprisingly, it should be highlighted that the glass transition temperatures of PhAs within modul-AAO are bulk-like ($T_{g,modul} \sim T_{g,bulk}$), which might indicate a negligible finite size effects of applied confinement despite the fact that the pore size of modulated templates changes within the range 19 nm < $D_p$ < 28 nm. This stresses the dominant role of surface effects on the behavior of confined materials.

Furthermore, we performed dielectric measurements. Representative dielectric loss, $\varepsilon''$, spectra obtained for bulk 2Ph1E and 5Ph1P and for samples infiltrated into const- and modul-AAO


https://doi.org/10.1021/acs.jpcc.2c05446
J. Phys. Chem. C 2022, 126, 18475−18489

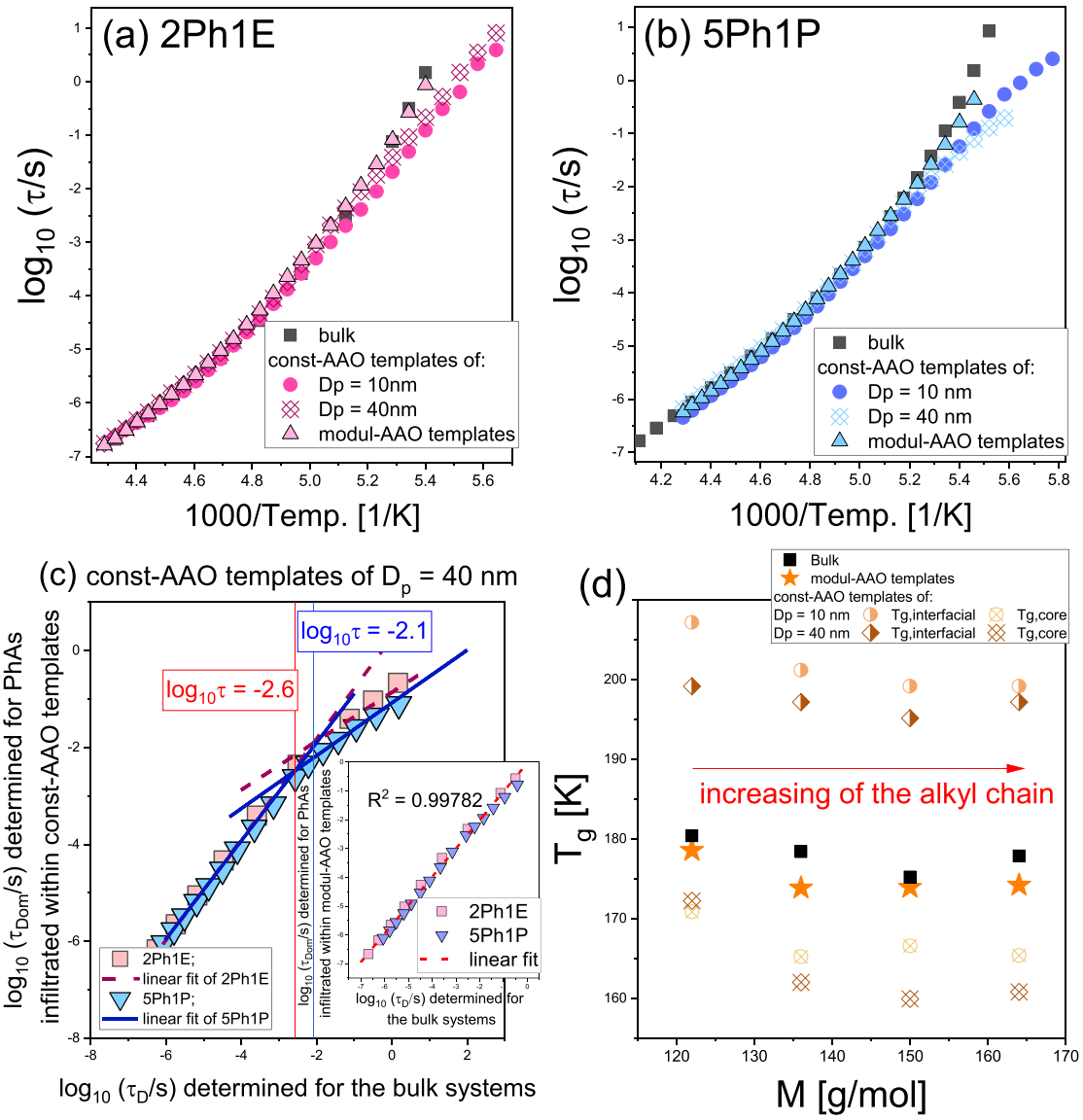


**Figure 6.** Temperature dependences of relaxation time ($\tau$) for 2Ph1E (a) and 5Ph1P (b) in the bulk and in 10 and 40 nm const-AAO and also modul-AAO membranes. (c) Debye relaxation times of the bulk versus those determined under confinement for both const-AAO of $D_p$ = 40 nm and modul-AAO (inset) templates. (d) Glass transition temperatures determined from dielectric data for all investigated systems.

membranes are shown in Figure 4. For all bulk samples, we can distinguish two relaxation processes, which shift toward lower frequencies as the temperature decreases: (i) dc-conductivity related with the ion transport (at lower frequencies) and (ii) prominent Debye-like ($D$) relaxation that dominates the recorded spectra (at higher frequencies, Figure 4a,d). Note that previous studies on bulk materials assigned this process as the $D$-relaxation, characterized by the Havriliak−Negami (HN) shape parameters close to one ($\alpha_{HN}$, $\beta_{HN} \approx 0.9$; see Figure S1 in the Supporting Information).[26] As mentioned in the Introduction, the presence of a dominant Debye-like relaxation is commonly observed in the dielectric spectra of various monoalcohols,[4,25,30,45] which most likely originates from the formation of associating structures.[13] It can be mentioned that, often, the dielectric spectra of monohydroxy alcohols also reveal a structural ($\alpha$) relaxation process, related to the glass transition in the high frequency region.[25,30,45] Interestingly, in our case we cannot detect the $\alpha$-process, suggesting that structural relaxation and the Debye mode are characterized by similar time scales. A similar scenario can be observed for PhAs confined within modul-AAO templates (see Figure 4c,f), in which the dielectric spectra are comparable to those of bulk systems exhibiting also the dc-conductivity process.

On the other hand, for alcohols confined in const-AAO membranes (see Figure 4b,e), we observe a presence of additional relaxation process located in the middle frequency range of significantly higher amplitude than the $D$-relaxation peak. Considering literature data published for the spatially restricted samples, this additional process might either be related to the motions of the molecules adsorbed to the pore walls (interfacial relaxation)[25,46] or the Maxwell−Wagner−Sillars (MWS) polarization (associated with heterogeneous dielectrics and connected with conductivity, permittivity, and geometry of phases).[32,47] However, taking into account the dominant amplitude of this process, we assigned this additional process as the MWS relaxation. Note that this process will not be discussed in this paper. In this context, one can mention that we do not observe any processes related to the dynamics of



https://doi.org/10.1021/acs.jpcc.2c05446
J. Phys. Chem. C 2022, 126, 18475−18489

molecules adsorbed (interfacial mode) on the pore walls. Herein, it should be commented that the presence of the additional interfacial process depends on many factors. As discussed in the literature, the appearance of this mode in loss spectra depends on the time scale of the mass exchange between interfacial and core molecules and experiment time.[48] Note that the interfacial process can be present or absent in the loss spectra when the exchange between both fractions is either fast or slow with respect to the time of the experiments, respectively. What is more, the interfacial process is also affected by the magnitude of dipole moment libration of immobilized molecules as well as long distance correlation between dipoles.

In order to better characterize the differences between the systems studied, we decided to compare the shape of the main relaxation process for each alcohol in the series; see Figure 5. As it can be seen for all examined materials, the shape of the dominant relaxation peak is broader (especially in the high-frequency region) in all confined systems when compared to the bulk sample. This agrees with the literature data, which clearly show that both $\alpha$ and Debye-like relaxations for various compounds exhibiting hydrogen interactions, i.e., PPG derivatives,[28,49,50] glycerol,[51] or monohydroxy alcohols[25] broaden under confinement regardless of the material (AAO/silica) due to an increase in the heterogeneity of the molecular mobility observed in the pores. Additionally for associating materials, the observed larger distribution of relaxation times for confined systems can be caused by a different time scale for $D$ and $\alpha$ processes because of changes in the hydrogen bond population under confinement.[4,52] Note that, due to the confinement-induced broadening, the observed loss peak is no longer a Debye-like relaxation; therefore, in the case of confined samples, we would assign this mode as a dominant relaxation process. Nevertheless, surprisingly, one can see that the broadest relaxation peak can be observed for PhAs infiltrated within modul-AAO templates independent of their molecular weight; see Figure 5. Note that for 3Ph1P and 4Ph1B, the main relaxation peak for samples within modul-AAO is even broader than those for PhAs within const-AAO templates of $D_p$ = 10 nm. This might indicate that the surface effects generated by the nanostructurization of the pore wall have a dominant role on the behavior of confined materials. Moreover, one can assume that the modulation-induced roughness of the inner pore surface is an additional source of heterogeneity within those systems, leading to a significant deviation in the population and strength of associates. Hence one can recall that the behavior described herein is consistent with the previous data on a series of PPGs incorporated within modul-AAO, which show that the $\alpha$-loss peak also broadens in the following manner: bulk → const-AAO → modul-AAO.[28]

In Figure 6a,b, we plotted the representative temperature dependences of bulk Debye-like and confined dominant processes relaxation times ($\tau$), obtained for 2Ph1E and 5Ph1P from the fitting the dielectric data with the HN function with an additional dc-conductivity term (see the Experimental Section). As one can see, the $\tau(T)$ of PhAs within both applied const-AAO membranes follows, at higher temperatures, the bulk-like VFT dependence, whereas upon cooling, $\tau(T)$ changes to an Arrhenius-like behavior at some specific temperature. This observed "change in the slope" is commonly observed for the confined systems[14,25,31,35−38] and often discussed in terms of either changes in the dynamical heterogeneities within the glass formers under confinement conditions[48,53] or the vitrification of the interfacial molecules.[35,38,54] In the case of the latter approach, it is assumed that after vitrification, the mobility of the interfacial fraction is limited and the systems enter isochoric conditions, which results in a change in the temperature dependence of relaxation times.[55,56] On the other hand, in the case of the $\tau(T)$ dependence for samples within modul-AAO templates, we observe that it is almost identical to that for the bulk, i.e., we do not see this characteristic kink as for const-AAO pores. Only at very low temperatures can we see a slight deviation from the bulk dependence, probably due to some finite size effects. This is further evidence for a very thin or even the absence of the interfacial layer of molecules in such systems. The same effect was also observed for a series of PPGs incorporated in modul-AAO templates.[28]

To better characterize these changes in $\tau(T)$ dependences among the series of studied alcohols, we plotted the Debye relaxation times ($\tau_D$) of the bulk versus those determined under confinement ($\tau_{Dom}$) for both const-AAO of $D_p$ = 40 nm (Figure 6c) and modul-AAO (the inset in Figure 6c). As one can see for const-AAO, such data presentation reveals a pronounced change in the slope. Note that the dashed and solid lines plotted in Figure 6c represent two linear fit functions (below and above the "kink") applied to find at what $\tau$ a change in the trend for presented dependences occurs. Interestingly, we can see that for PhAs with "even" lengths of alkyl chain (4Ph1B and 2Ph1E), this change takes place at $\log(\tau_D) \approx -2.1$, whereas, for PhAs with "odd" lengths of alkyl chain (3Ph1P and 5Ph1P), the dependence breaks at $\log(\tau_D) \approx -2.6$. Interestingly, the changes in slopes of $\tau(T)$ evolutions occur at a comparable relaxation time, although there are some manifestations of the "odd−even" effect. In this context, one can recall recent dielectric studies on the dynamics of a series of aliphatic monoalcohols, 2E1H, 2E1B, and 5M3H, infiltrated into native and silanized silica templates of $D_p$ = 4−8 nm,[25] which also reported that the changes in the slope of their $\tau(T)$ dependences occurs at similar $\log(\tau_D) \sim -1$, independent of their chemical structure and silica pores modification (inducing a variation in the interfacial energies between a native and silanized template). This behavior was discussed in terms of two approaches: (1) alcohol molecules prefer to form intermolecular H-bonds, rather than bonds with the template, independent of the pore functionalization,[57] and (2) all materials are characterized by the similar sensitivity of the structural process to the density fluctuations.[49] One can see that those data agree with the ones presented herein; however, for examined phenyl alcohols confined in const-AAO templates, this specific deviation of $\tau(T)$ dependences occurs at higher temperatures when compared to the above-mentioned aliphatic one. In contrast, for phenyl alcohols infiltrated within modul-AAO membranes, we observe a perfect linear dependence ($R^2$ = 0.998) of the plotted relationship; see the inset in Figure 6c. This supports the previously mentioned bulk-like behavior of modul materials.

In the next step, we determined the glass transition temperatures for all the studied systems from the dielectric data. In order to determine $T_g$ for the bulk and modul-AAO systems, the temperature dependence curves of the relaxation times, due to their exponential nature, were fitted using a Vogel−Fulcher−Tamman (VFT) function:[58−60]

$$\tau_D = \tau_\infty \exp\left(\frac{D_T T_0}{T - T_0}\right) \quad (3)$$

where $\tau_\infty$ is the relaxation time at finite temperature, $T_0$ is the temperature when $\tau$ goes to infinity and $D_T$ is the fragility



https://doi.org/10.1021/acs.jpcc.2c05446
J. Phys. Chem. C 2022, 126, 18475−18489

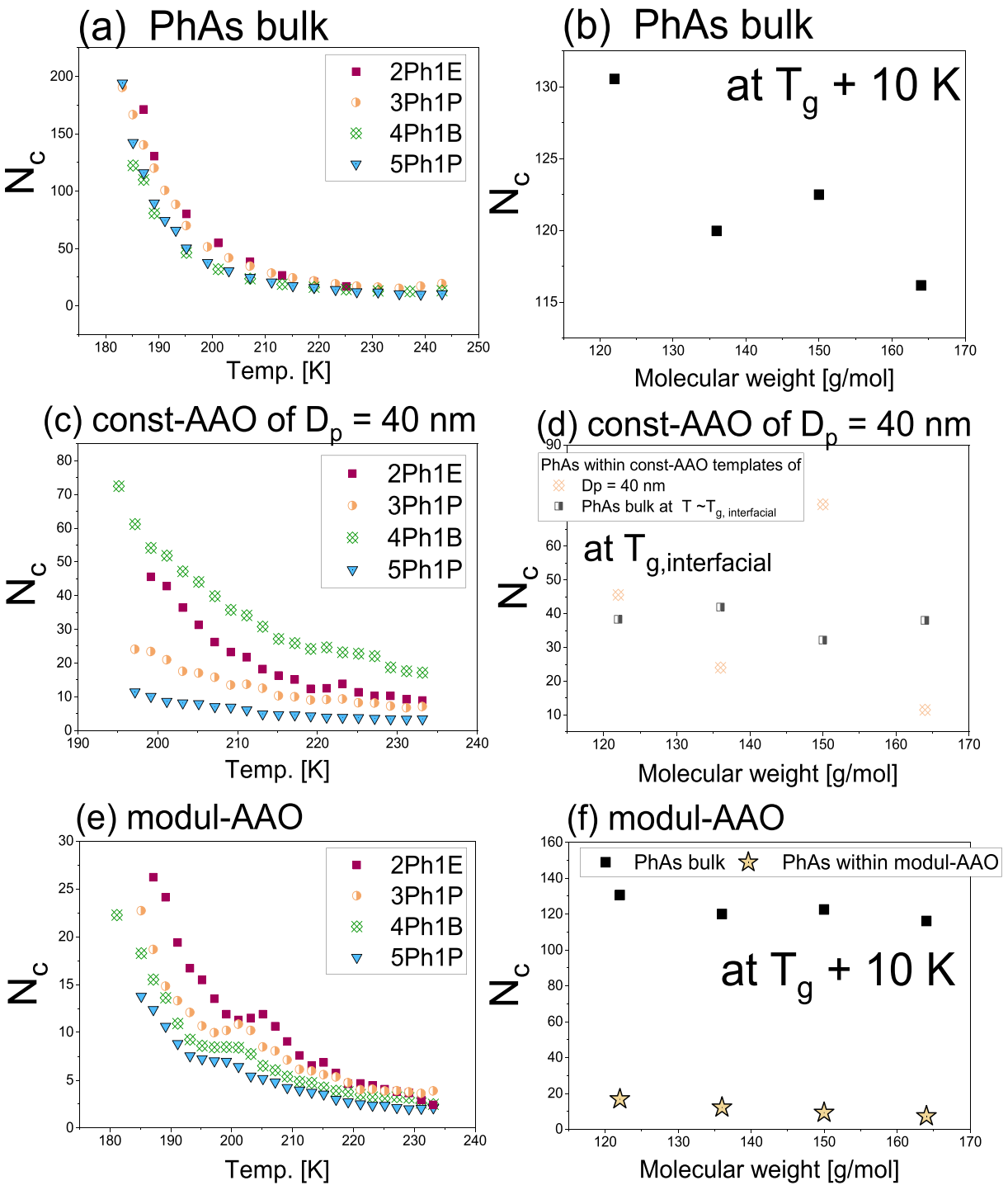


**Figure 7.** Number of molecules dynamically correlated during the relaxation process ($N_c$) calculated for studied alcohols in bulk (a), 40 nm const-AAO (c), and modul-AAO (e) membranes. Comparison of $N_c$ values, determined for a given temperature, between investigated systems (b, d, f).

parameter. $T_g$ values of the bulks were determined as the temperature at which $\tau$ = 100 s by extrapolating the VFT fits. Herein it should be mentioned that similar results were obtained from fitting the data with the Avramov equation (see Figure S2 in the Supporting Information). To determine $T_{g,core}$ for systems confined in const-AAO templates, their $\tau_{Dom}(T)$ dependences below $T_{g,interfacial}$ (after the kink), were fitted with the Arrhenius equation (due to their linear character):

$$\tau_D = \tau_\infty \exp\left(\frac{\Delta E}{k_b T}\right) \quad (4)$$

where $k_b$ is the Boltzmann constant and $\Delta E$ is the activation energy. Similarly, as in the case of bulk and modul-AAO, $T_{g,core}$ was determined from the Arrhenius fit extrapolation up to $\tau$ = 100 s. The determined values of glass transition temperatures for all systems, from the dielectric measurements are shown in Figure 6d and listed in Table 1. As illustrated in Figure 6d, $T_g$ values for bulk and modul-AAO membranes are comparable,



https://doi.org/10.1021/acs.jpcc.2c05446
J. Phys. Chem. C 2022, 126, 18475−18489

independent of the alcohol chain length. $T_{g,interfacial}$ of interfacial molecules for samples confined in const-AAO membranes were determined from the kink in the plot shown in Figure 6c or alternatively form the Stickel approach.[61] For details, see the Supporting Information file. The temperature dependences of the $S$ parameter are shown in Figure S3. As it can be seen, all $S(T)$ dependences for the pores began to deviate from the bulk behavior at $T_{g,interfacial}$, which values agree with both the high glass transition temperature determined from calorimetric measurements and analysis presented in Figure 6c. Additionally, there is good agreement between values of $T_g$ determined from both dielectric and calorimetric data (see Table 1), although there are some differences in the values of $T_g$ values determined from both experimental methods reaching $\Delta T_g \approx 10-12$ K (see Table 1). Those differences might occur due to different heating rates applied in both techniques. Note that, comparison of calorimetric $T_g$ values obtained at different heating rates (Figure 3a,b) shows values of $T_g$ determined for 5 K/min are comparable to those obtained from the BDS. Nevertheless, it should be mentioned that despite those differences, the $T_g(M)$ dependences obtained from dielectric data are essentially the same as those determined from DSC measurements. It is also important to stress that in the case of const-AAO templates, both $T_{g,interfacial}$ and $T_{g,core}$ are significantly shifted when compared to the bulk material. Moreover, both $T_g$ values decrease with the elongation of the alkyl chain; see Figure 6d. However, $T_{g,interfacial}$ is a few kelvins higher for $D_p = 10$ nm than for $D_p = 40$ nm, which seems to be consistent with the literature data. Interestingly, the same effect is observed for $T_{g,core}$.

Furthermore, we decided to monitor the impact of the applied confinement on the dynamical heterogeneity of studied alcohols, for that purpose, we calculated the number of correlated molecules involved in the observed relaxation process, $N_c$, using the following equation proposed by Berthier et al.[62,63] and further modified by Capaccioli et al.:[64]

$$N_c = \chi_4^{max} \approx \frac{k_b}{\Delta C_p}\left(\frac{\partial \Phi(t)}{\partial T}\right)^2 = \frac{k_b}{\Delta C_p}\left(\frac{\beta_{KWW}}{e}\right)^2\left(\frac{\partial \ln \tau}{\partial \ln T}\right)^2 \quad (5)$$

where: $\Delta C_p$ is the heat capacity change at $T_g$ (per molecule), $\beta_{KWW}$ is the stretching parameter of Kohlrausch−Williams−Watts function, and $e$ is Euler's number. Note that assuming that the maximal value of the dynamic susceptibility $\chi_4^{max}$ was preidentified with $N_c$ on a time scale of $t \sim \tau_\alpha$ and the KWW function $[\exp(-(t/\tau_\alpha)^{\beta_{KWW}})]$ is used to describe $\Phi(t)$; the number of molecules that are dynamically correlated during the structural relaxation of supercooled liquids, $N_c$, can be simplified as reported in ref 64. Additionally, $\beta_{KWW}$ was calculated from HN shape parameters, $\alpha_{HN}$ and $\beta_{HN}$, using the following formula:[65]

$$\alpha_{HN}\beta_{HN} = \beta_{KWW}^{1.23} \quad (6)$$

Determined temperature dependences of $N_c$ are presented in Figure 7. Note that for const-AAO systems, we only calculated $N_c$ at the higher temperature range (above $T_{g,interfacial}$) and use $\Delta C_p$ at $T_{g,core}$ in eq 6. As shown in Figure 7a, we observe an exponential increase in $N_c$ values with decreasing temperature for all the studied alcohols. In addition, the number of correlated molecules appears to be similar for all investigated samples; see Figure 7b. In general, the $N_c$ parameter changes in the range $N_c = 115-130$; however, it is clearly seen that the values for 2Ph1E and 4Ph1B are higher than for 3Ph1P and 5Ph1P, which might be another manifestation of the "odd−even" effect. Nevertheless, it should be mentioned that determined values of $N_c$ as well as their temperature dependence are more or less similar to those obtained for other bulk systems exhibiting hydrogen bonds: 1,6-anhydro-$\beta$-D-glucose ($N_c \sim 100$)[66] and salol ($N_c \sim 100$).[67] For comparison, one can add that in the case of van der Waals materials, $N_c$ reaches the following values near $T_g$, i.e., $N_c \approx 20-250$ (polymers),[68] $N_c \sim 500$ (propylene carbonate)[67] and $N_c \sim 400$ (posaconazole).[69]

For PhAs confined in const-AAO membranes illustrated in Figure 7c, the picture is quite different than for the bulks. Interestingly, there are significant differences between alcohols containing even (2Ph1E, 4Ph1B) and odd (3Ph1P, 5Ph1P) number of alkyl groups, both in terms of the $N_c$ value and its temperature dependence. As shown in Figure 7d, the number of correlated molecules in samples infiltrated within const-AAO membranes of $D_p = 40$ nm changes according to the "odd−even" effect. Moreover, one can see that the $N_c$ parameter is lower (by 10−30) than that for bulks at the same temperature conditions. Note that there is one exception, as for 4Ph1B, the value of $N_c$ is higher for confined systems when compared to the bulk at the same temperature. One can assume that the reduced values of correlated molecules is most likely caused by the finite size effects of applied confinement, which limits the characteristic length scale of associating molecules. This effect agrees also with the data reporting significant reduction of the number of molecules involved in the formation of the chain like structures.

On the other hand, for PhAs confined in modul-AAO membranes (see Figure 7e), $N_c(T)$ decreases with the elongation of alkyl chain, which is more similar to that of the bulk than the one observed for const-AAO systems. However, surprisingly, values of $N_c$ are significantly lower than those of the macroscale material. Due to the bulk-like behavior of the modul-AAO systems, one would expect the $N_c$ values to be close to those determined for the bulk. Interestingly, the number of correlated molecules is almost 10 times lower than those determined for the bulk ($N_{c,modul-AAO} \sim 10-14$; see Figure 7f). Those values are even smaller than $N_c$ determined for PhAs incorporated within const-AAO templates of and $D_p = 40$ nm. This is quite surprising behavior as, in the case of bulk materials, it is expected that the variation in $N_c$ should affect the relaxation times, $\tau$. Nevertheless, in the case of confined materials, this might not be the case. However, we observed a decrease of $N_c$ for examined porous materials, the $\tau_D(T)$ of PhAs infiltrate within modul-AAO remains bulk-like. We assume that this is a result of a specific counterbalance between confinement-induced factors. Note that the presence of a constrained medium used to generate the nanoscale confinement conditions affects significantly the molecular dynamics of nanomaterials due to the two main factors, (1) finite size (where 19 nm < $D_p$ < 28 nm) and (2) surface effects (including modulation-induced roughness of the inner pore walls). Both of them affect the density packing and molecular rearrangement in a different manner. Therefore, we assume that both of them have their own contribution to the bulk-like dynamics observed in the case of modul-AAO membranes despite a reduction of $N_c$. It should be highlighted that to the best of our knowledge this is the first study that follows the change in the number of correlated molecules involved in the observed relaxation process of samples infiltrated into porous templates of modulated values of pore sizes. Therefore, this issue requires further studies.

Lastly, we examine the variation in the glass transition temperatures as a function of wettability (quantified by contact


https://doi.org/10.1021/acs.jpcc.2c05446
J. Phys. Chem. C 2022, 126, 18475−18489

angle, $\theta$) and interfacial energy, $\gamma_{SL}$. One can recall that, recently, there have been an increasing number of reports linking macroscopic parameters, i.e., interfacial energy, with the magnitude of the confinement effects.[31,70] As it was shown for different glass formers incorporated into AAO templates, there was a linear increase of glass transition temperatures, assigned as $\Delta T_{g,interfacial} = T_{g,interfacial} - T_{g,bulk}$ and $\Delta T_{g,core} = T_{g,bulk} - T_{g,core}$ with the increase of $\gamma_{SL}$.[46,67] Therefore, we decided to check if the observed deviation of $T_g$ values of confined phenyl alcohols also scales with $\theta$ and $\gamma_{SL}$. Note that values of $\gamma_{SL}$ were calculated using Young's equation:

$$\gamma_{SL} = \gamma_S - \gamma_L \cos\theta \quad (7)$$

where $\gamma_{SL}$ is the interfacial energy, $\gamma_S$ is the surface energy ($\gamma_S$ = 58,97 mN/m, for $Al_2O_3$, $T$ = 298 K), $\gamma_L$ is surface tension of liquids, and $\theta$ is the contact angle. Detailed information about the calculations can be found in refs 34 and 71. Values of all parameters, $\theta$, $\gamma_L$, and $\gamma_{SL}$, determined for all studied alcohols are listed in Table 2. As it can be seen for the contact angle and surface tension of liquids, both variables decrease with the increase of the molecular weight of examined PhAs. Note that values of the contact angle decrease from $\theta \sim 14.1-13.3°$ (for both 2Ph1P and 3Ph1P) to $\theta \sim 9.5°$ (for 4Ph1B and 5Ph1P). However, interestingly, the interfacial energy remains constant ($\gamma_{SL} \sim 21$ mN/m) regardless of the length of the chain. The $\gamma_{SL}$ (and $\theta$) dependences of $\Delta T_{g,interfacial}$ and $\Delta T_{g,core}$ for all examined confined systems are shown in Figure 8. As observed, all samples are characterized by similar $\Delta T_{g,interfacial}$ and $\Delta T_{g,core}$ independent of the chemical structure of the examined PhAs. This finding is in agreement with the general trend reported by Alexandris et al.[31] since similar values of $\gamma_{SL}$ lead to a comparable deviation of the glass transition temperatures. The same scenario can be also observed for $\Delta T_g(\theta)$ dependences; see the insets in Figure 8. However, herein, two groups of points for the short (2Ph1E and 3Ph1P) and long alkyl chain (4Ph1B and 5Ph1P) are visible. Interestingly, the same trend can be detected for both const- and modul-AAO membranes, blue solid lines in the insets in Figure 8. On the other hand, both $\Delta T_{g,core}$ and $\Delta T_{g,interfacial}$ increase with increasing pore diameter. The observed relationships between $\Delta T_g$ and $D_p$ are in agreement with those reported for PPGs.[49]

**Table 2. Contact Angle ($\theta$), Surface Tension of Liquids ($\gamma_L$) and Interfacial Energy ($\gamma_{SL}$) Determined for All Studied Alcohols**[a]

| sample | $\theta$ [deg] | $\gamma_L$ [mN/m][26] | $\gamma_{SL}$ [mN/m] |
|---|---|---|---|
| 2Ph1E | 14.1 | 38.8 | 21.1 |
| 3Ph1P | 13.3 | 38.3 | 21.7 |
| 4Ph1B | 9.3 | 37.3 | 22.2 |
| 5Ph1P | 9.9 | 37.0 | 22.5 |

[a]All presented parameters were determined at $T$ = 298 K.

## IV. CONCLUSIONS

In this paper, we monitored the impact of nanoscale confinement on the behavior of a series phenyl alcohols using BDS and DSC techniques. In the case of the compounds confined within const-AAO membranes, we observed the presence of the double glass transition phenomenon in the calorimetric data, typically reported for infiltrated materials. On the other hand, application of the membranes with a modulated pore size (which might be considered to cause an increased roughness of inner pore walls), had a significant impact on the behavior of confined PhAs. In

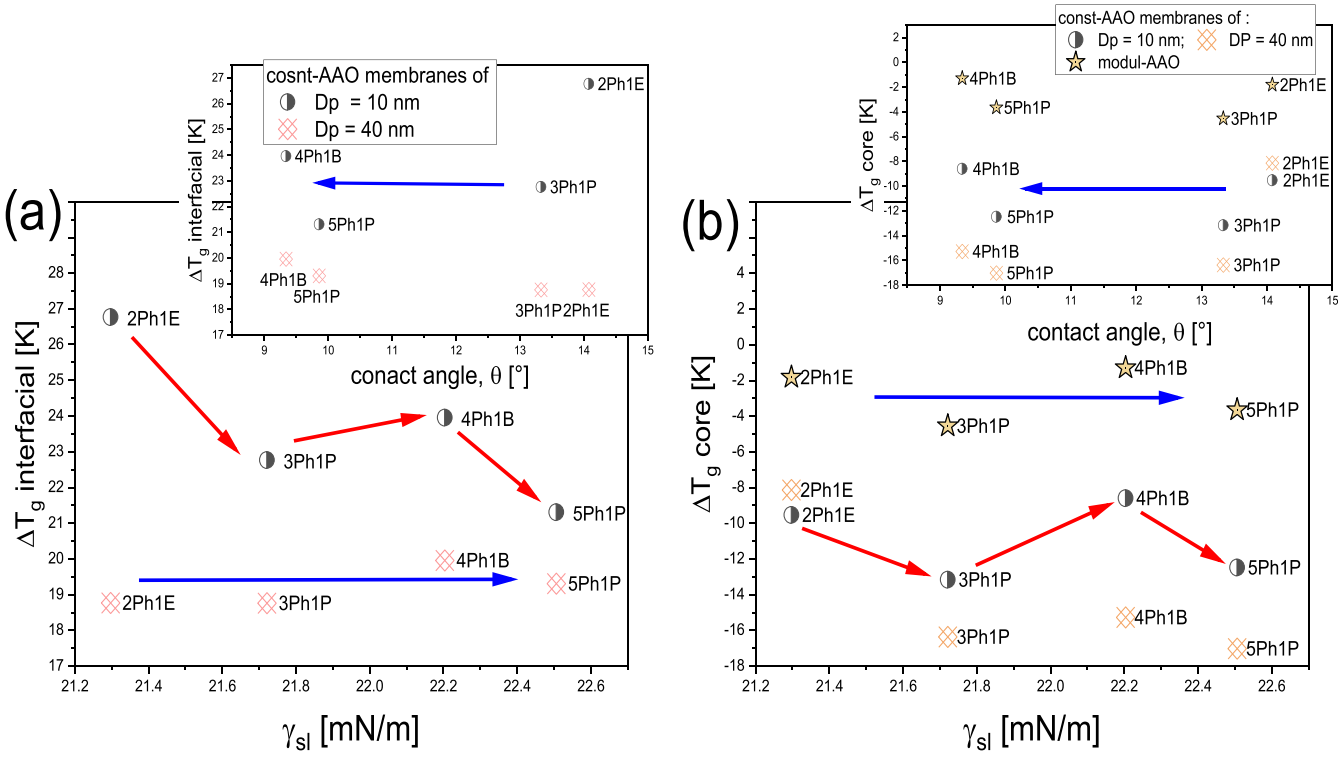


**Figure 8.** Interfacial energy, $\gamma_{SL}$, dependences of the shift on the interfacial and core glass transition temperature quantified as $\Delta T_{g,interfacial} = T_{g,interfacial} - T_{g,bulk}$ and $\Delta T_{g,core} = T_{g,bulk} - T_{g,core}$ for all examined confined systems. Insets in panels (a, b): contact angle, $\theta$, dependences of $\Delta T_{g,interfacial}$ and $\Delta T_{g,core}$ for all examined confined systems. Solid blue lines indicate the increase of molecular weight of studied materials.



https://doi.org/10.1021/acs.jpcc.2c05446
J. Phys. Chem. C 2022, 126, 18475−18489

contrast to const-AAO membranes, materials within modul-AAO exhibited bulk-like character for a number of parameters investigated, i.e., lack of second glass transition, high agreement between $T_{g,modul}$ and $T_{g,bulk}$. Furthermore, for all bulk and confined samples, the recorded dielectric spectra were dominated by a pronounced relaxation process (which for the bulk is Debye-like). Interestingly, in the case of confined phenyl alcohols, we did not observe any additional relaxation processes, either structural $\alpha$ relaxation or an interfacial process related to dynamics of molecules interacting with the pore walls. This implies no impact on the applied confinement on the time scale between $D$ and $\alpha$ processes. However, a comparison of the dielectric loss peak shapes indicated that they are no longer a Debye type since significant broadening of the dielectric response function was noted for all confined samples. Importantly, the width of the dominant process was the largest for PhAs infiltrated within modul-AAO membranes. It suggests the greatest dynamical heterogeneity in these systems. Moreover, for PhAs infiltrated in const-AAO templates, a change in the $\tau(T)$ dependence from exponential (VFT) to linear (Arrhenius) can be observed. Surprisingly, the samples in modul-AAO membranes revealed a bulk-like behavior in the whole range of studied temperatures. On the other hand, values of dynamically correlated molecules involved in the relaxation process ($N_c$) calculated for modul-AAO systems were the lowest from all investigated samples ($N_c \approx 20$ molecules near $T_g$) despite the observed bulk-like $\tau_D(T)$ dependence. We believe that the reduction of $N_c$ results from the two major factors finite size effects and modulation-induced roughness of inner pore walls. Interestingly, we found that the modulated pore size of the modul-AAO template has a significant impact on the Debye relaxation reflecting the population of hydrogen bonds. Moreover, the performed contact angle and surface tension measurements showed that there is a correlation between the direction and magnitude of the confinement effect and $\theta$ (as well as $\gamma_{SL}$), as it was previously reported in the literature in the case of polymers.

## ■ ASSOCIATED CONTENT

### Supporting Information

The Supporting Information is available free of charge at https://pubs.acs.org/doi/10.1021/acs.jpcc.2c05446.

Temperature dependences of HN shape parameters and the Stickel ($S$) parameter, as well as temperature dependences of relaxation time for bulk 2Ph1E and 5Ph1P fitted to both VFT and Avramov equations (PDF)

## ■ AUTHOR INFORMATION


### Corresponding Author

**Magdalena Tarnacka** − *August Chełkowski Institute of Physics, University of Silesia in Katowice, 41-500 Chorzów, Poland;* orcid.org/0000-0002-9444-3114; Email: magdalena.tarnacka@us.edu.pl, magdalena.tarnacka@smcebi.edu.pl

### Authors

**Adam Górny** − *August Chełkowski Institute of Physics, University of Silesia in Katowice, 41-500 Chorzów, Poland*

**Sara Zimny** − *Institute of Chemistry, University of Silesia in Katowice, 40-006 Katowice, Poland;* orcid.org/0000-0003-3812-1353

**Monika Geppert-Rybczyńska** − *Institute of Chemistry, University of Silesia in Katowice, 40-006 Katowice, Poland;* orcid.org/0000-0002-7112-9624

**Agnieszka Brzózka** − *Faculty of Chemistry, Department of Physical Chemistry and Electrochemistry, Jagiellonian University, 30-387 Krakow, Poland*

**Grzegorz D. Sulka** − *Faculty of Chemistry, Department of Physical Chemistry and Electrochemistry, Jagiellonian University, 30-387 Krakow, Poland;* orcid.org/0000-0001-7431-617X

**Marian Paluch** − *August Chełkowski Institute of Physics, University of Silesia in Katowice, 41-500 Chorzów, Poland;* orcid.org/0000-0002-7280-8557

**Kamil Kamiński** − *August Chełkowski Institute of Physics, University of Silesia in Katowice, 41-500 Chorzów, Poland;* orcid.org/0000-0002-5871-0203

Complete contact information is available at: https://pubs.acs.org/10.1021/acs.jpcc.2c05446


### Notes

The authors declare no competing financial interest.

## ■ ACKNOWLEDGMENTS

M.T. and K.K. are thankful for financial support from the Polish National Science Centre within the OPUS project (Dec. no 2019/33/B/ST3/00500).

## ■ REFERENCES


(1) Jindal, A.; Vasudevan, S. Hydrogen Bonding in the Liquid State of Linear Alcohols: Molecular Dynamics and Thermodynamics. *J. Phys. Chem. B* **2020**, *124* (17), 3548−3555.

(2) Böhmer, R.; Gainaru, C.; Richert, R. Structure and Dynamics of Monohydroxy Alcohols—Milestones towards Their Microscopic Understanding, 100 Years after Debye. *Phys. Rep.* **2014**, *545* (4), 125−195.

(3) Lombardo, D.; Kiselev, M. A.; Magazù, S.; Calandra, P. Amphiphiles Self-Assembly: Basic Concepts and Future Perspectives of Supramolecular Approaches. *Adv. Condens. Matter Phys.* **2015**, *2015*, 1−22.

(4) Böhmer, T.; Gabriel, J. P.; Richter, T.; Pabst, F.; Blochowicz, T. Influence of Molecular Architecture on the Dynamics of H-Bonded Supramolecular Structures in Phenyl-Propanols. *J. Phys. Chem. B* **2019**, *123* (51), 10959−10966.

(5) Pothoczki, S.; Pethes, I.; Pusztai, L.; Temleitner, L.; Ohara, K.; Bakó, I. Properties of Hydrogen-Bonded Networks in Ethanol-Water Liquid Mixtures as a Function of Temperature: Diffraction Experiments and Computer Simulations. *J. Phys. Chem. B* **2021**, *125* (23), 6272−6279.

(6) Kholmanskiy, A. Hydrogen Bonds and Dynamics of Liquid Water and Alcohols. *J. Mol. Liq.* **2021**, *325*, 115237.

(7) Soszka, N.; Hachuła, B.; Tarnacka, M.; Kaminska, E.; Pawlus, S.; Kaminski, K.; Paluch, M. Is a Dissociation Process Underlying the Molecular Origin of the Debye Process in Monohydroxy Alcohols. *J. Phys. Chem. B* **2021**, *125* (11), 2960−2967.

(8) Wang, Y.; Griffin, P. J.; Holt, A.; Fan, F.; Sokolov, A. P. Observation of the Slow, Debye-like Relaxation in Hydrogen-Bonded Liquids by Dynamic Light Scattering. *J. Chem. Phys.* **2014**, *140* (10), 104510.

(9) Wieth, P.; Vogel, M. Dynamical and Structural Properties of Monohydroxy Alcohols Exhibiting a Debye Process. *J. Chem. Phys.* **2014**, *140* (14), 144507.

(10) Ngai, K. L.; Grzybowska, K.; Grzybowski, A.; Kaminska, E.; Kaminski, K.; Paluch, M.; Capaccioli, S. Recent Advances in Fundamental Understanding of Glass Transition. *J. Non. Cryst. Solids* **2008**, *354* (47−51), 5085−5088.

(11) Capaccioli, S.; Paluch, M.; Prevosto, D.; Wang, L.-M.; Ngai, K. L. Many-Body Nature of Relaxation Processes in Glass-Forming Systems. *J. Phys. Chem. Lett.* **2012**, *3* (6), 735−743.
(12) Gabriel, J.; Pabst, F.; Helbling, A.; Böhmer, T.; Blochowicz, T. Nature of the Debye-Process in Monohydroxy Alcohols: 5-Methyl-2-Hexanol Investigated by Depolarized Light Scattering and Dielectric Spectroscopy. *Phys. Rev. Lett.* **2018**, *121* (3), 035501.
(13) Gainaru, C.; Meier, R.; Schildmann, S.; Lederle, C.; Hiller, W.; Rössler, E. A.; Böhmer, R. Nuclear-Magnetic-Resonance Measurements Reveal the Origin of the Debye Process in Monohydroxy Alcohols. *Phys. Rev. Lett.* **2010**, *105* (25), 258303.
(14) Ananiadou, A.; Papamokos, G.; Steinhart, M.; Floudas, G. Effect of Confinement on the Dynamics of 1-Propanol and Other Monohydroxy Alcohols. *J. Chem. Phys.* **2021**, *155* (18), 184504.
(15) Nowok, A.; Dulski, M.; Jurkiewicz, K.; Grelska, J.; Szeremeta, A. Z.; Grzybowska, K.; Pawlus, S. Molecular Stiffness and Aromatic Ring Position − Crucial Structural Factors in the Self-Assembly Processes of Phenyl Alcohols. *J. Mol. Liq.* **2021**, *335*, 116426.
(16) Nowok, A.; Dulski, M.; Grelska, J.; Szeremeta, A. Z.; Jurkiewicz, K.; Grzybowska, K.; Musiał, M.; Pawlus, S. Phenyl Ring: A Steric Hindrance or a Source of Different Hydrogen Bonding Patterns in Self-Organizing Systems? *J. Phys. Chem. Lett.* **2021**, *12* (8), 2142−2147.
(17) Johari, G. P.; Kalinovskaya, O. E.; Vij, J. K. Effects of Induced Steric Hindrance on the Dielectric Behavior and H Bonding in the Supercooled Liquid and Vitreous Alcohol. *J. Chem. Phys.* **2001**, *114* (10), 4634.
(18) Okuchi, T.; Cody, G. D.; Mao, H.; Hemley, R. J. Hydrogen Bonding and Dynamics of Methanol by High-Pressure Diamond-Anvil Cell NMR. *J. Chem. Phys.* **2005**, *122* (24), 244509.
(19) Gromnitskaya, E. L.; Danilov, I. V.; Lyapin, A. G.; Brazhkin, V. V. Elastic Properties of Liquid and Glassy Propane-Based Alcohols under High Pressure: The Increasing Role of Hydrogen Bonds in a Homologous Family. *Phys. Chem. Chem. Phys.* **2019**, *21* (5), 2665−2672.
(20) Fragiadakis, D.; Roland, C. M.; Casalini, R. Insights on the Origin of the Debye Process in Monoalcohols from Dielectric Spectroscopy under Extreme Pressure Conditions. *J. Chem. Phys.* **2010**, *132* (14), 144505.
(21) Arencibia, A.; Taravillo, M.; Pérez, F. J.; Núñez, J.; Baonza, V. G. Effect of Pressure on Hydrogen Bonding in Liquid Methanol. *Phys. Rev. Lett.* **2002**, *89* (19), 195504.
(22) Hachuła, B.; Kamińska, E.; Koperwas, K.; Wrzalik, R.; Jurkiewicz, K.; Tarnacka, M.; Scelta, D.; Fanetti, S.; Pawlus, S.; Paluch, M.; Kamiński, K. A Study of O H···O Hydrogen Bonds along Various Isolines in 2-Ethyl-1-Hexanol. Temperature or Pressure - Which Parameter Controls Their Behavior? *Spectrochim. Acta Part A Mol. Biomol. Spectrosc.* **2022**, *283*, 121726.
(23) Gainaru, C.; Schildmann, S.; Böhmer, R. Surface and Confinement Effects on the Dielectric Relaxation of a Monohydroxy Alcohol. *J. Chem. Phys.* **2011**, *135* (17), 174510.
(24) Kipnusu, W. K.; Elsayed, M.; Kossack, W.; Pawlus, S.; Adrjanowicz, K.; Tress, M.; Mapesa, E. U.; Krause-Rehberg, R.; Kaminski, K.; Kremer, F. Confinement for More Space: A Larger Free Volume and Enhanced Glassy Dynamics of 2-Ethyl-1-Hexanol in Nanopores. *J. Phys. Chem. Lett.* **2015**, *6* (18), 3708−3712.
(25) Talik, A.; Tarnacka, M.; Geppert-Rybczyńska, M.; Hachuła, B.; Bernat, R.; Chrzanowska, A.; Kaminski, K.; Paluch, M. Are Hydrogen Supramolecular Structures Being Suppressed upon Nanoscale Confinement? The Case of Monohydroxy Alcohols. *J. Colloid Interface Sci.* **2020**, *576*, 217−229.
(26) Soszka, N.; Hachuła, B.; Tarnacka, M.; Kamińska, E.; Grelska, J.; Jurkiewicz, K.; Geppert-Rybczyńska, M.; Wrzalik, R.; Grzybowska, K.; Pawlus, S.; Paluch, M.; Kamiński, K. The Impact of the Length of Alkyl Chain on the Behavior of Benzyl Alcohol Homologues − the Interplay between Dispersive and Hydrogen Bond Interactions. *Phys. Chem. Chem. Phys.* **2021**, *23* (41), 23796−23807.
(27) Sulka, G. D.; Brzózka, A.; Zaraska, L.; Jaskuła, M. Through-Hole Membranes of Nanoporous Alumina Formed by Anodizing in Oxalic Acid and Their Applications in Fabrication of Nanowire Arrays. *Electrochim. Acta* **2010**, *55* (14), 4368−4376.
(28) Tarnacka, M.; Wojtyniak, M.; Brzózka, A.; Talik, A.; Hachuła, B.; Kamińska, E.; Sulka, G. D.; Kaminski, K.; Paluch, M. Unique Behavior of Poly(Propylene Glycols) Confined within Alumina Templates Having a Nanostructured Interface. *Nano Lett.* **2020**, *20* (8), 5714−5719.
(29) Iacob, C.; Sangoro, J. R.; Papadopoulos, P.; Schubert, T.; Naumov, S.; Valiullin, R.; Kärger, J.; Kremer, F. Charge Transport and Diffusion of Ionic Liquids in Nanoporous Silica Membranes. *Phys. Chem. Chem. Phys.* **2010**, *12* (41), 13798.
(30) Kipnusu, W. K.; Kossack, W.; Iacob, C.; Jasiurkowska, M.; Rume Sangoro, J.; Kremer, F. Molecular Order and Dynamics of Tris(2-Ethylhexyl)Phosphate Confined in Uni-Directional Nanopores. *Zeitschrift für Phys. Chemie* **2012**, *226* (7−8), 797−805.
(31) Alexandris, S.; Papadopoulos, P.; Sakellariou, G.; Steinhart, M.; Butt, H. J.; Floudas, G. Interfacial Energy and Glass Temperature of Polymers Confined to Nanoporous Alumina. *Macromolecules* **2016**, *49* (19), 7400−7414.
(32) Kremer, F.; Schönhals, A.*Broadband Dielectric Spectroscopy*; Springer, 2003
(33) Wandschneider, A.; Lehmann, J. K.; Heintz, A. Surface Tension and Density of Pure Ionic Liquids and Some Binary Mixtures with 1-Propanol and 1-Butanol. *J. Chem. Eng. Data* **2008**, *53* (2), 596−599.
(34) Feder-Kubis, J.; Geppert-Rybczyńska, M.; Musiał, M.; Talik, E.; Guzik, A. Exploring the Surface Activity of a Homologues Series of Functionalized Ionic Liquids with a Natural Chiral Substituent: (−)-Menthol in a Cation. *Colloids Surfaces A Physicochem. Eng. Asp.* **2017**, *529*, 725−732.
(35) Szklarz, G.; Adrjanowicz, K.; Tarnacka, M.; Pionteck, J.; Paluch, M. Confinement-Induced Changes in the Glassy Dynamics and Crystallization Behavior of Supercooled Fenofibrate. *J. Phys. Chem. C* **2018**, *122* (2), 1384−1395.
(36) Tarnacka, M.; Talik, A.; Kamińska, E.; Geppert-Rybczyńska, M.; Kaminski, K.; Paluch, M. The Impact of Molecular Weight on the Behavior of Poly(Propylene Glycol) Derivatives Confined within Alumina Templates. *Macromolecules* **2019**, *52* (9), 3516−3529.
(37) Talik, A.; Tarnacka, M.; Minecka, A.; Hachula, B.; Grelska, J.; Jurkiewicz, K.; Kaminski, K.; Paluch, M.; Kaminska, E. Anormal Thermal History Effect on the Structural Dynamics of Probucol Infiltrated into Porous Alumina. *J. Phys. Chem. C* **2021**, *125* (7), 3901−3912.
(38) Adrjanowicz, K.; Kolodziejczyk, K.; Kipnusu, W. K.; Tarnacka, M.; Mapesa, E. U.; Kaminska, E.; Pawlus, S.; Kaminski, K.; Paluch, M. Decoupling between the Interfacial and Core Molecular Dynamics of Salol in 2D Confinement. *J. Phys. Chem. C* **2015**, *119* (25), 14366−14374.
(39) Talik, A.; Tarnacka, M.; Geppert-Rybczyńska, M.; Hachuła, B.; Kaminski, K.; Paluch, M. Impact of Confinement on the Dynamics and H-Bonding Pattern in Low-Molecular Weight Poly(Propylene Glycols). *J. Phys. Chem. C* **2020**, *124* (32), 17607−17621.
(40) Cheng, S.; McKenna, G. B. Nanoconfinement Effects on the Glass Transition and Crystallization Behaviors of Nifedipine. *Mol. Pharmaceutics* **2019**, *16* (2), 856−866.
(41) Park, J.-Y.; McKenna, G. B. Size and Confinement Effects on the Glass Transition Behavior of Polystyrene/ o -Terphenyl Polymer Solutions. *Phys. Rev. B* **2000**, *61* (10), 6667−6676.
(42) Kuon, N.; Milischuk, A. A.; Ladanyi, B. M.; Flenner, E. Self-Intermediate Scattering Function Analysis of Supercooled Water Confined in Hydrophilic Silica Nanopores. *J. Chem. Phys.* **2017**, *146* (21), 214501.
(43) Avramov, I.; Gutzow, I. Heating Rate and Glass Transition Temperature. *J. Non. Cryst. Solids* **1988**, *104* (1), 148−150.
(44) Schawe, J. E. K.; Löffler, J. F. Existence of Multiple Critical Cooling Rates Which Generate Different Types of Monolithic Metallic Glass. *Nat. Commun.* **2019**, *10* (1), 1337.
(45) Büning, T.; Lueg, J.; Bolle, J.; Sternemann, C.; Gainaru, C.; Tolan, M.; Böhmer, R. Connecting Structurally and Dynamically

Detected Signatures of Supramolecular Debye Liquids. *J. Chem. Phys.* **2017**, *147* (23), 234501.
(46) He, F.; Wang, L.-M.; Richert, R. Dynamics of Supercooled Liquids in the Vicinity of Soft and Hard Interfaces. *Phys. Rev. B* **2005**, *71* (14), 144205.
(47) Yao, Y.; Suzuki, Y.; Seiwert, J.; Steinhart, M.; Frey, H.; Butt, H.-J. J.; Floudas, G. Capillary Imbibition, Crystallization, and Local Dynamics of Hyperbranched Poly(Ethylene Oxide) Confined to Nanoporous Alumina. *Macromolecules* **2017**, *50* (21), 8755−8764.
(48) Arndt, M.; Stannarius, R.; Gorbatschow, W.; Kremer, F. Dielectric Investigations of the Dynamic Glass Transition in Nanopores. *Phys. Rev. E* **1996**, *54* (5), 5377−5390.
(49) Talik, A.; Tarnacka, M.; Grudzka-Flak, I.; Maksym, P.; Geppert-Rybczynska, M.; Wolnica, K.; Kaminska, E.; Kaminski, K.; Paluch, M. The Role of Interfacial Energy and Specific Interactions on the Behavior of Poly(Propylene Glycol) Derivatives under 2D Confinement. *Macromolecules* **2018**, *51* (13), 4840−4852.
(50) Tarnacka, M.; Kaminski, K.; Mapesa, E. U.; Kaminska, E.; Paluch, M. Studies on the Temperature and Time Induced Variation in the Segmental and Chain Dynamics in Poly(Propylene Glycol) Confined at the Nanoscale. *Macromolecules* **2016**, *49* (17), 6678−6686.
(51) Talik, A.; Tarnacka, M.; Wojtyniak, M.; Kaminska, E.; Kaminski, K.; Paluch, M. The Influence of the Nanocurvature on the Surface Interactions and Molecular Dynamics of Model Liquid Confined in Cylindrical Pores. *J. Mol. Liq.* **2020**, *298*, 111973.
(52) Soszka, N.; Hachuła, B.; Tarnacka, M.; Grelska, J.; Jurkiewicz, K.; Geppert-Rybczyńska, M.; Wrzalik, R.; Grzybowska, K.; Pawlus, S.; Paluch, M.; Kamiński, K. Aromaticity Effect on Supramolecular Aggregation. Aromatic vs. Cyclic Monohydroxy Alcohols. *Spectrochim. Acta Part A Mol. Biomol. Spectrosc.* **2022**, *276*, 121235.
(53) Uhl, M.; Fischer, J. K. H.; Sippel, P.; Bunzen, H.; Lunkenheimer, P.; Volkmer, D.; Loidl, A. Glycerol Confined in Zeolitic Imidazolate Frameworks: The Temperature-Dependent Cooperativity Length Scale of Glassy Freezing. *J. Chem. Phys.* **2019**, *150* (2), 024504.
(54) Tarnacka, M.; Dulski, M.; Geppert-Rybczyńska, M.; Talik, A.; Kamińska, E.; Kamiński, K.; Paluch, M. Variation in the Molecular Dynamics of DGEBA Confined within AAO Templates above and below the Glass-Transition Temperature. *J. Phys. Chem. C* **2018**, *122* (49), 28033−28044.
(55) Adrjanowicz, K.; Kaminski, K.; Koperwas, K.; Paluch, M. Negative Pressure Vitrification of the Isochorically Confined Liquid in Nanopores. *Phys. Rev. Lett.* **2015**, *115* (26), 1−5.
(56) Tarnacka, M.; Kipnusu, W. K.; Kaminska, E.; Pawlus, S.; Kaminski, K.; Paluch, M. The Peculiar Behavior of the Molecular Dynamics of a Glass-Forming Liquid Confined in Native Porous Materials-the Role of Negative Pressure. *Phys. Chem. Chem. Phys.* **2016**, *18* (34), 23709−23714.
(57) Ghoufi, A.; Hureau, I.; Morineau, D.; Renou, R.; Szymczyk, A. Confinement of Tert -Butanol Nanoclusters in Hydrophilic and Hydrophobic Silica Nanopores. *J. Phys. Chem. C* **2013**, *117* (29), 15203−15212.
(58) Vogel, H. Temperatura Bhangigkeitgesetz Der Viskosität von Flüssigkeiten. *J. Phys. Z.* **1921**, *22*, 645−646.
(59) Fulcher, G. S. Analysis of Recent Measurements of the Viscosity of Glasses. *J. Am. Ceram. Soc.* **1925**, *8*, 339−355.
(60) Tammann, G.; Hesse, W. Die Abhängigkeit Der Viscosität von Der Temperatur Bie Unterkühlten Flüssigkeiten. *Z. Anorg. Allg. Chem.* **1926**, *156*, 245−257.
(61) Stickel, F.; Fischer, E. W.; Richert, R. Dynamics of Glass-Forming Liquids. I. Temperature-Derivative Analysis of Dielectric Relaxation Data. *J. Chem. Phys.* **1995**, *102* (15), 6251−6257.
(62) Berthier, L.; Biroli, G.; Bouchaud, J.-P.; Cipelletti, L.; Masri, D. El; L'Hôte, D.; Ladieu, F.; Pierno, M. Direct Experimental Evidence of a Growing Length Scale Accompanying the Glass Transition. *Science (80-.)* **2005**, *310* (5755), 1797−1800.
(63) Berthier, L. Dynamic Heterogeneity in Amorphous Materials. *Physics (College. Park. Md)* **2011**, *4*, 42.
(64) Capaccioli, S.; Ruocco, G.; Zamponi, F. Dynamically Correlated Regions and Configurational Entropy in Supercooled Liquids. *J. Phys. Chem. B* **2008**, *112* (34), 10652−10658.
(65) Alvarez, F.; Alegra, A.; Colmenero, J. Relationship between the Time-Domain Kohlrausch-Williams-Watts and Frequency-Domain Havriliak-Negami Relaxation Functions. *Phys. Rev. B* **1991**, *44* (14), 7306−7312.
(66) Madejczyk, O.; Kaminski, K.; Kaminska, E.; Jurkiewicz, K.; Tarnacka, M.; Burian, A.; Paluch, M. Interplay between the Static Ordering and Dynamical Heterogeneities Determining the Dynamics of Rotation and Ordinary Liquid Phases in 1,6-Anhydro-$\beta$-D-Glucose. *Sci. Rep.* **2017**, *7* (February), 1−7.
(67) Fragiadakis, D.; Casalini, R.; Roland, C. M. Density Scaling and Dynamic Correlations in Viscous Liquids. *J. Phys. Chem. B* **2009**, *113* (40), 13134−13137.
(68) Rijal, B.; Delbreilh, L.; Saiter, A. Dynamic Heterogeneity and Cooperative Length Scale at Dynamic Glass Transition in Glass Forming Liquids. *Macromolecules* **2015**, *48* (22), 8219−8231.
(69) Adrjanowicz, K.; Kaminski, K.; Wlodarczyk, P.; Grzybowska, K.; Tarnacka, M.; Zakowiecki, D.; Garbacz, G.; Paluch, M.; Jurga, S. Molecular Dynamics of the Supercooled Pharmaceutical Agent Posaconazole Studied via Differential Scanning Calorimetry and Dielectric and Mechanical Spectroscopies. *Mol. Pharmaceutics* **2013**, *10* (10), 3934−3945.
(70) Politidis, C.; Alexandris, S.; Sakellariou, G.; Steinhart, M.; Floudas, G. Dynamics of Entangled Cis −1,4-Polyisoprene Confined to Nanoporous Alumina. *Macromolecules* **2019**, *52* (11), 4185−4195.
(71) Talik, A.; Tarnacka, M.; Geppert-Rybczynska, M.; Minecka, A.; Kaminska, E.; Kaminski, K.; Paluch, M. Impact of the Interfacial Energy and Density Fluctuations on the Shift of the Glass-Transition Temperature of Liquids Confined in Pores. *J. Phys. Chem. C* **2019**, *123* (9), 5549−5556.


https://doi.org/10.1021/acs.jpcc.2c05446
*J. Phys. Chem. C* 2022, 126, 18475−18489